DR-FAIRNESS: DYNAMIC DATA RATIO ADJUSTMENT FOR FAIR TRAINING ON REAL AND GENERATED DATA

Anonymous authors
Paper under double-blind review

ABSTRACT

Fair visual recognition has become critical for preventing demographic disparity. A major cause of model unfairness is the imbalanced representation of different groups in training data. Recently, several works aim to alleviate this issue using generated data. However, these approaches often use generated data to obtain similar amounts of data across groups, which is not optimal for achieving high fairness due to different learning difficulties and generated data qualities across groups. To address this issue, we propose a novel adaptive sampling approach that leverages both real and generated data for fairness. We design a bilevel optimization that finds the optimal data sampling ratios among groups and between real and generated data while training a model. The ratios are dynamically adjusted considering both the model's accuracy as well as its fairness. To efficiently solve our non-convex bilevel optimization, we propose a simple approximation to the solution given by the implicit function theorem. Extensive experiments show that our framework achieves state-of-the-art fairness and accuracy on the CelebA and ImageNet People Subtree datasets. We also observe that our method adaptively relies less on the generated data when it has poor quality.

1 INTRODUCTION

Model fairness in visual recognition is becoming essential to prevent discriminatory predictions over demographics. Recently, numerous unfairness issues have been reported (Wang et al., 2020; Najibi, 2020), and several fair image classification approaches have been proposed that do not discriminate against specific groups such as gender, age, or skin color (Ramaswamy et al., 2021; Roh et al., 2021).

With the rapid progress in deep generative learning (Karras et al., 2020; Dhariwal & Nichol, 2021), there is a new research direction to improve fairness by augmenting training data with generated data. Recent breakthroughs in generative learning make generated data practical enough to use in real-world applications (OpenAI, 2022), and many high-quality pre-trained generative models are now open to the public (Rombach et al., 2022), which obviates the need to train such models ourselves. Thus, generated data is increasingly used to improve model performances, including fairness. From a fairness perspective, generated data complements real data by making it more diverse. For example, if a specific group's data is collected from a limited data source that does not have the full data distribution, that group may be discriminated in model training due to the bias (Mehrabi et al., 2021). In this case, generated data can be used to supplement that underrepresented group.

However, most fair training approaches that use generated data simply generate similar amounts of data across groups (Ramaswamy et al., 2021; Choi et al., 2020), which may not be optimal to improve group fairness such as equalized odds (Hardt et al., 2016) and demographic parity (Feldman et al., 2015). Such suboptimality could originate from 1) the learning difficulty differences across groups and 2) the potential bias (i.e., typically in the form of missing modes) and quality issues in the generated data that can hurt the accuracy and fairness of the model under training. Therefore, it is essential to find the right mix of generated and real data for the best accuracy and fairness.

In this paper, we *harness the potential of both real and generated data via adaptive sampling* to improve group fairness while minimizing accuracy degradation. To this end, we design a new sampling approach called Dr-Fairness (**D**ynamic Data **R**atio Adjustment for **Fairness**) that adaptively adjusts data ratios among groups and between real and generated data over iterations, as in Figure 1a.

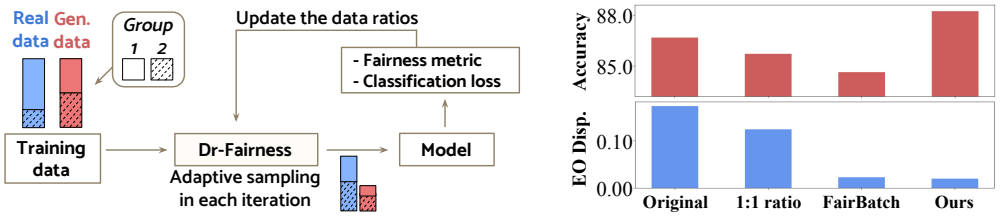

(a) Framework overview. (b) Accuracy and fairness performances.

Figure 1: (a) Our framework iteratively updates the data ratios among groups and between real and generated data based on the fairness and accuracy of the intermediate model. (b) Performances on CelebA, using `gender` as the group attribute and `age` as the label attribute. Compared to the original model, the 1:1 ratio baseline (Ramaswamy et al., 2021) does not significantly improve group fairness, measured through equalized odds (EO) disparity. FairBatch (Roh et al., 2021) shows high fairness by adaptively selecting real data only, but loses accuracy. In comparison, Dr-Fairness (ours) achieves high fairness, while not sacrificing accuracy.

Table 1: Functionality comparison of algorithms.

Method	Uses generated data	Finds the optimal group ratio	Finds the optimal real & gen. data ratio	Utilizes accuracy for ratio updates
1:1 ratio	✓	✗	✗	✗
FairBatch	✗	✓	✗	✗
Dr-Fairness	✓	✓	✓	✓

In Table 1, we compare the unique properties of Dr-Fairness against two representative methods: 1) an equal ratio baseline (1:1 ratio) (Ramaswamy et al., 2021) that uses generated data and 2) a fairness-aware adaptive sampling baseline (FairBatch) (Roh et al., 2021) that finds the optimal group ratio for fairness only using real data. We can see that Dr-Fairness subsumes the two baselines and improves them by also optimizing the ratio between real and generated data and utilizing accuracy for ratio updates.

To perform adaptive sampling systematically, we design a novel bilevel optimization problem along with an efficient algorithm for solving it. Our bilevel optimization consists of 1) an outer optimization that adjusts data sampling ratios considering both fairness and accuracy and 2) an inner optimization that minimizes the standard empirical risk on both real and generated data, given the current sampling ratios. Although various exact algorithms have been proposed to solve bilevel optimizations (Maclaurin et al., 2015), they often scale poorly in our scenario with large models and data. We thus propose an approximate algorithm that uses the implicit function theorem (Krantz & Parks, 2002) and identity-matrix approximation (Luketina et al., 2016) to efficiently compute the gradient of our bilevel optimization. Specifically, instead of computing the expensive inverse Hessian matrix, we approximate it with a simple diagonal identity matrix.

Experiments on CelebA (Liu et al., 2015) and ImageNet People Subtree (Yang et al., 2020) show that our approach achieves the state-of-the-art fairness and accuracy performances. For instance, Figure 1b highlights our results on CelebA, where our framework largely outperforms FairBatch, which only uses real data and the 1:1 ratio baseline – see Sec. 3 for comparisons using more baselines and other fairness metrics, which show consistent results. On the ImageNet People Subtree classification problem, which represents a large-scale real-world scenario, we achieve better accuracies than the best baseline, with an absolute improvement of 5–9%, while obtaining similar fairness scores. We also observe that our framework adaptively relies less on the generated data when it has poor quality.

Summary of Contributions: (1) We propose Dr-Fairness, a novel adaptive sampling framework for fair training that enjoys the potential of both real and generated data. (2) To perform adaptive sampling systematically, we formulate a bilevel optimization to train fair and accurate models on real and generated data. (3) We also design an approximate algorithm based on the implicit function theorem and identity-matrix approximation to efficiently solve our optimization. (4) We perform extensive experiments on CelebA and ImageNet People Subtree to show that Dr-Fairness achieves the state-of-the-art accuracy and fairness. (5) Finally, we believe that our work reveals the importance of using generated data together with real data to improve model fairness.

2 Framework

In this section, we first formulate a bilevel optimization problem for optimizing sampling ratios for real and generated data. We then design a new algorithm that efficiently solves the optimization problem. Throughout this paper, we use the following notations and fairness definitions.

Notations Let $x \in \mathbb{X}$ be the input feature, and let $y \in \mathbb{Y}$ and $\hat{y} \in \mathbb{Y}$ be the true label and the predicted label, respectively. Let $z \in \mathbb{Z}$ be a sensitive group attribute, e.g., gender, age, or skin

color. Let m be the total number of training samples, and $m_{y,z}$ be the number of samples in the set $\{i : \mathrm{y}_i = y, \mathrm{z}_i = z\}$ with label y and group label z. Similarly, $m_{y,\star} := |\{i : \mathrm{y}_i = y\}|$ and $m_{\star,z} := |\{i : \mathrm{z}_i = z\}|$. Let $\boldsymbol{w}$ be the model weights, and the overall empirical risk is given by $L(\boldsymbol{w}) = \frac{1}{m}\sum_i \ell(\mathrm{y}_i, \hat{\mathrm{y}}_i)$, where $\ell(\cdot)$ represents the loss function. Let $L_{y,z}(\boldsymbol{w})$ be the empirical risk over samples in the set $\{i : \mathrm{y}_i = y, \mathrm{z}_i = z\}$, i.e., $L_{y,z}(\boldsymbol{w}) := \frac{1}{m_{y,z}}\sum_{i:\mathrm{y}_i=y,\mathrm{z}_i=z} \ell(\mathrm{y}_i, \hat{\mathrm{y}}_i)$. Finally, let $L^{\text{real}}(\cdot)$ and $L^{\text{gen}}(\cdot)$ be the empirical risks on real data and generated data, respectively.

Fairness Definitions For the method design, we focus on two prominent group fairness definitions: equalized odds (EO) (Hardt et al., 2016) and demographic parity (DP) (Feldman et al., 2015). EO is satisfied when the accuracies conditioned on the true label are the same for different groups (i.e., $\Pr(\hat{\mathrm{y}} = y|\mathrm{y} = y, \mathrm{z} = z_1) = \Pr(\hat{\mathrm{y}} = y|\mathrm{y} = y, \mathrm{z} = z_2), \forall y \in \mathbb{Y}, z_1, z_2 \in \mathbb{Z}$). DP is satisfied when the positive prediction rates are the same for the groups (i.e., $\Pr(\hat{\mathrm{y}} = 1|\mathrm{z} = z_1) = \Pr(\hat{\mathrm{y}} = 1|\mathrm{z} = z_2), \forall z_1, z_2 \in \mathbb{Z}$), where DP is designed for binary classifications (i.e., $y \in \{0, 1\}$) with a favorable label class (e.g., "approval" in loan decision).

Generated Data In general, any synthetic data, including data from deep generative models, can be considered generated data for fair training. Here, the key role of the generated data in algorithmic fairness is supporting the limited subset of the real data. Also, we implicitly assume that the domains of the generated data and real data are the same, but the distributions of the two data can be different. For example, if the real data represents human faces, then we assume the generated data also contains human faces. However, generated data may have a fairer distribution than real data. In this paper, we assume we can get group-specific generated data by using conditional image generation techniques (Nie et al., 2021; Dhariwal & Nichol, 2021) – see details in Secs. 3 and B.3.

2.1 Bilevel Optimization for Fairness with Real and Generated Data

To design an adaptive sampling strategy on real and generated data, we first formulate a bilevel optimization for training fair and accurate models. The bilevel optimization consists of inner and outer objectives: 1) we maintain the standard empirical risk minimization (ERM) in the inner problem, and 2) we capture the desired fairness properties in the outer problem. The bilevel formulation allows us to support prominent group fairness metrics and utilize generated data for fairness. Moreover, through this formulation, we can achieve the desired fairness properties while keeping the standard model training process without re-configuring the model architecture or loss functions.

We now explain how our optimization improves group fairness and accuracy together by using both real and generated data. The outer objective aims to find the optimal data ratios among sensitive groups and between real and generated data to minimize the fairness and accuracy losses on the real data distribution. Given the current data ratios, the inner objective runs a weighted ERM with both real and generated data. We can support various prominent group fairness metrics by modifying the outer objective and the constraints. As an illustration, we state our bilevel optimization w.r.t. EO as follows (see the DP version in Sec. A.1):

$$\min_{\boldsymbol{\lambda},\boldsymbol{\mu}} \max_{y\in\mathbb{Y},z_1,z_2\in\mathbb{Z}} \{|L^{\text{real}}_{y,z_1}(\boldsymbol{w}(\boldsymbol{\lambda},\boldsymbol{\mu})) - L^{\text{real}}_{y,z_2}(\boldsymbol{w}(\boldsymbol{\lambda},\boldsymbol{\mu}))|\} + k \sum_{y\in\mathbb{Y},z\in\mathbb{Z}} \frac{m_{y,z}}{m} L^{\text{real}}_{y,z}(\boldsymbol{w}(\boldsymbol{\lambda},\boldsymbol{\mu})),$$
$$\boldsymbol{w}(\boldsymbol{\lambda},\boldsymbol{\mu}) = \arg\min_{\boldsymbol{w}} \sum_{y\in\mathbb{Y},z\in\mathbb{Z}} \frac{m_{y,\star}}{m} \lambda_{y,z}\{\mu_{y,z} L^{\text{real}}_{y,z}(\boldsymbol{w}) + (1-\mu_{y,z}) L^{\text{gen}}_{y,z}(\boldsymbol{w})\},$$
$$\text{s.t.} \quad \boldsymbol{\lambda} \in [0,1], \boldsymbol{\mu} \in [0,1], \sum_{z\in\mathbb{Z}} \lambda_{y,z} = 1, \forall y \in \mathbb{Y},$$

where $\lambda_{y,z}$ is the ratio for group z in class y, $\mu_{y,z}$ is the ratio for real data in the (y, z)-class, and $\boldsymbol{\lambda}$ and $\boldsymbol{\mu}$ are the sets of all $\lambda_{y,z}$ and $\mu_{y,z}$, respectively. In the outer objective, the first term indicates the fairness loss, and second term indicates accuracy loss. The hyperparameter k tunes the importance of the two losses. We note that the $\lambda_{y,z}$ and $\mu_{y,z}$ values are the data ratios within one mini-batch. Thus, among all samples in the real and generated data, our framework serves mini-batches according to $\lambda_{y,z}$ and $\mu_{y,z}$. Here, we can capture the EO disparity as the maximum of the loss differences in different groups within the same label (i.e., $\max |L^{\text{real}}_{y,z_1}(\boldsymbol{w}) - L^{\text{real}}_{y,z_2}(\boldsymbol{w})|$) – see the details in Sec. A.2.

Through the above formulation, the amount of generated data is automatically adjusted to augment the real data. One problem with only using real data is that there can be an accuracy degradation of the model due to over-sampling minority groups for better fairness. Generating data for these groups can prevent the model's overfitting and lessen the accuracy degradation.

2.2 ALGORITHM

We now design our algorithm to solve the above bilevel optimization. In this section, we first describe how to efficiently approximate our optimization by utilizing the implicit function theorem (Krantz & Parks, 2002) and adapting identity-matrix approximation (Luketina et al., 2016) in a fairness setting. We then introduce the overall training procedure, and show the validity of our approximate algorithm on synthetic data.

Algorithm Design Solving bilevel optimization is known to be challenging (Liu et al., 2021), especially when the objectives are non-convex as in our problem. Thus, we resort to stochastic gradient descent to find the optimal parameters of the bilevel optimization gradually. To obtain the gradients, we first convert our optimization into the unconstrained version:

$$\min_{\boldsymbol{\lambda},\boldsymbol{\mu}} \max_{y\in\mathbb{Y},z_1,z_2\in\mathbb{Z}} \{|L^{\text{real}}_{y,z_1}(\boldsymbol{w}(\boldsymbol{\lambda},\boldsymbol{\mu})) - L^{\text{real}}_{y,z_2}(\boldsymbol{w}(\boldsymbol{\lambda},\boldsymbol{\mu}))|\} + k\sum_{y\in\mathbb{Y},z\in\mathbb{Z}} \frac{m_{y,z}}{m} L^{\text{real}}_{y,z}(\boldsymbol{w}(\boldsymbol{\lambda},\boldsymbol{\mu})),$$

$$\boldsymbol{w}(\boldsymbol{\lambda},\boldsymbol{\mu}) = \arg\min_{\boldsymbol{w}} \sum_{y\in\mathbb{Y},z\in\mathbb{Z}} \frac{m_{y,\star}}{m}\sigma_y(\lambda_{y,z})\{S(\mu_{y,z})L^{\text{real}}_{y,z}(\boldsymbol{w}) + (1-S(\mu_{y,z}))L^{\text{gen}}_{y,z}(\boldsymbol{w})\},$$

where $\sigma_y(\lambda_{y,z}) := \exp(\lambda_{y,z})/\sum_{z_i}\exp(\lambda_{y,z_i})$ (i.e., the softmax function), and $S(\mu_{y,z}) := 1/(1+\exp(-\mu_{y,z}))$ (i.e., the sigmoid function). Denoting the outer and inner objectives as $f_{\text{outer}}(\boldsymbol{\lambda},\boldsymbol{\mu},\boldsymbol{w}(\boldsymbol{\lambda},\boldsymbol{\mu}))$ and $f_{\text{inner}}(\boldsymbol{\lambda},\boldsymbol{\mu},\boldsymbol{w})$ respectively, the inner optimization $\boldsymbol{w}(\boldsymbol{\lambda},\boldsymbol{\mu}) = \arg\min_{\boldsymbol{w}} f_{\text{inner}}(\boldsymbol{\lambda},\boldsymbol{\mu},\boldsymbol{w})$ can be solved efficiently using SGD-like algorithms. The main question is how to solve the outer optimization. We can state the gradient of f_{outer} w.r.t. $\boldsymbol{\lambda}$ as follows:

$$\frac{df_{\text{outer}}}{d\boldsymbol{\lambda}} = \underbrace{\frac{\partial f_{\text{outer}}}{\partial\boldsymbol{\lambda}}}_{\text{Term A}} + \underbrace{\frac{\partial f_{\text{outer}}}{\partial\boldsymbol{w}(\boldsymbol{\lambda},\boldsymbol{\mu})}}_{\text{Term B}} \times \underbrace{\frac{\partial\boldsymbol{w}(\boldsymbol{\lambda},\boldsymbol{\mu})}{\partial\boldsymbol{\lambda}}}_{\text{Term C}}, \tag{1}$$

where Term A and Term B are the direct gradients w.r.t. $\boldsymbol{\lambda}$ and $\boldsymbol{w}(\boldsymbol{\lambda},\boldsymbol{\mu})$, respectively, and Term C is the best-response Jacobian. Note that $\boldsymbol{w}(\boldsymbol{\lambda},\boldsymbol{\mu})$ is the best-response of model weights.

In Eq. 1, the best-response Jacobian is hard to directly compute. Although various algorithms have been proposed to *explicitly* find the best-response Jacobian, most of them require propagating the entire history of the gradients (Maclaurin et al., 2015), which is very time-consuming. Instead, we *implicitly* measure the best-response Jacobian using the implicit function theorem (Krantz & Parks, 2002). This approach does not need to investigate the entire gradient history (Rajeswaran et al., 2019; Lorraine et al., 2020) and builds on the assumption that the inner optimization has converged to a local minimum, i.e., $\frac{\partial f_{\text{inner}}}{\partial\boldsymbol{w}} = 0$. Using this assumption, we can convert the best-response Jacobian into the multiplication of two matrices (see more details in Corollary 2 of Sec. A.3):

$$\frac{df_{\text{outer}}}{d\boldsymbol{\lambda}} = \frac{\partial f_{\text{outer}}}{\partial\boldsymbol{\lambda}} + \frac{\partial f_{\text{outer}}}{\partial\boldsymbol{w}(\boldsymbol{\lambda},\boldsymbol{\mu})} \times -[\frac{\partial^2 f_{\text{inner}}}{\partial\boldsymbol{w}\partial\boldsymbol{w}}]^{-1} \times \frac{\partial^2 f_{\text{inner}}}{\partial\boldsymbol{w}\partial\boldsymbol{\lambda}}. \tag{2}$$

However, obtaining the inverse Hessian (i.e., $[\partial^2 f_{\text{inner}}/\partial\boldsymbol{w}\partial\boldsymbol{w}]^{-1}$) in Eq. 2 is also computationally expensive. Thus, we consider the identity matrix approximation (Luketina et al., 2016; Finn et al., 2017; Geng et al., 2021) that replaces the inverse Hessian with the identity matrix. Despite its simplicity, such approximation may be valid for neural networks with normalization layers that make the Hessian matrix diagonally dominant (e.g. BatchNorm), and in practice, it often performs on par with other approximation methods in various applications (Raiko et al., 2012; Pedregosa, 2016; Liu et al., 2018; Wilder et al., 2019; Fung et al., 2022). Given this, we can rewrite Eq. 2 simply as:

$$\frac{df_{\text{outer}}}{d\boldsymbol{\lambda}} \approx \frac{\partial f_{\text{outer}}}{\partial\boldsymbol{\lambda}} - \frac{\partial f_{\text{outer}}}{\partial\boldsymbol{w}(\boldsymbol{\lambda},\boldsymbol{\mu})} \times \frac{\partial^2 f_{\text{inner}}}{\partial\boldsymbol{w}\partial\boldsymbol{\lambda}}, \tag{3}$$

where the second term on the right-hand side is efficiently computed via vector-Jacobian product (Paszke et al., 2017). Similarly, we can also approximate the gradient of f_{outer} w.r.t. $\boldsymbol{\mu}$.

Overall Training Process We now describe the overall training process in Algo. 1. We first initialize the model parameters and the data ratios, and for each iteration, we then get a minibatch from Dr-Fairness (Algo. 2). In Algo. 2, we first update the data ratios among groups ($\boldsymbol{\lambda}$) and between real and generated data ($\boldsymbol{\mu}$) by calculating $\frac{df_{\text{outer}}}{d\boldsymbol{\lambda}}$ and $\frac{df_{\text{outer}}}{d\boldsymbol{\mu}}$ as in Eq. 3. We then draw a minibatch according to $\sigma_y(\boldsymbol{\lambda})$ and $S(\boldsymbol{\mu})$. Note that the batch sampling with $\sigma_y(\boldsymbol{\lambda})$ and $S(\boldsymbol{\mu})$ provides an unbiased estimator of the weighted ERM in our inner optimization (Roh et al., 2021). Finally, we update the model parameters $\boldsymbol{w}$ with the given minibatch. Here we can optionally use an exponential moving average (EMA) that averages the model parameters $\boldsymbol{w}$ for improving training stability.

Algorithm 1: Model Training with Dr-Fairness

Input: real data $(x_{\text{real}}, y_{\text{real}}, z_{\text{real}})$, generated data $(x_{\text{gen}}, y_{\text{gen}}, z_{\text{real}})$
$\boldsymbol{d}_{\text{real}}, \boldsymbol{d}_{\text{gen}} \leftarrow (x_{\text{train}}, y_{\text{train}}, z_{\text{real}}), (x_{\text{gen}}, y_{\text{gen}}, z_{\text{real}})$
$\boldsymbol{w} \leftarrow$ initial model parameters
$\boldsymbol{\lambda}, \boldsymbol{\mu} \leftarrow$ initialize sampling ratio logits
Get current sampling ratios $\sigma_y(\boldsymbol{\lambda}), S(\boldsymbol{\mu})$
for *each iteration* **do**
  minibatch=`Dr-Fairness`$(\boldsymbol{w}, \boldsymbol{d}_{\text{real}}, \boldsymbol{d}_{\text{gen}}, \boldsymbol{\lambda}, \boldsymbol{\mu})$
  Update $\boldsymbol{w}$ according to the minibatch (optionally with exponential moving average (EMA))
Output : model parameters $\boldsymbol{w}$

Algorithm 2: Dr-Fairness

Input: model parameters $\boldsymbol{w}$, data $\boldsymbol{d}_{\text{real}}$ and $\boldsymbol{d}_{\text{gen}}$, group ratio $\boldsymbol{\lambda}$, real data ratio $\boldsymbol{\mu}$
Calculate f_{outer} and f_{inner} according to $\boldsymbol{w}$, $\boldsymbol{d}_{\text{real}}$, $\boldsymbol{d}_{\text{gen}}$, $\boldsymbol{\lambda}$, and $\boldsymbol{\mu}$
Get $\frac{df_{\text{outer}}}{d\boldsymbol{\lambda}}$ and $\frac{df_{\text{outer}}}{d\boldsymbol{\mu}}$ as in Eq. 3
Update $\boldsymbol{\lambda}$ by $\frac{df_{\text{outer}}}{d\boldsymbol{\lambda}}$ and $\boldsymbol{\mu}$ by $\frac{df_{\text{outer}}}{d\boldsymbol{\mu}}$ using optimizers (e.g., Adam)
Draw a minibatch w.r.t. $\sigma_y(\boldsymbol{\lambda})$, $S(\boldsymbol{\mu})$
Output : minibatch

Validity of Our Algorithm We empirically verify how close the solutions from our approximation strategy are to the optimal ones. To this end, we follow the synthetic binary setting in Roh et al. (2021), where FairBatch has a theoretical guarantee to find the optimal group ratios, and compare the optimized group ratios of Dr-Fairness and FairBatch – see details on the setup in Sec. A.4. Note that in this synthetic setting, we set the fairness metric to equal opportunity (i.e., a relaxed version of EO that focuses on the positive label) and only use the real data to optimize the group ratios $\boldsymbol{\lambda}$, as FairBatch cannot handle $\boldsymbol{\mu}$ for the generated data. Ideally, if the approximation error in our method is small, Dr-Fairness should obtain the same group ratios and performance as FairBatch.

Figure 2 shows that our algorithm converges to similar group ratios to those in FairBatch, although the key ideas of the two algorithms on updating the group ratio are very different. Also, the two algorithms have the similar fairness scores (0.012 equal opportunity disparity for both). These results imply that our approximations are good enough to find reasonable solutions, which is consistent with the observations in other applications (Lorraine et al., 2020; Luketina et al., 2016). In the next section, we will show that Dr-Fairness achieves much higher accuracy with similar or better fairness than FairBatch on real-world datasets, as our algorithm scales to multiple groups and labels and is capable of harnessing the potential of both real and generated data. We note that although FairBatch is known to have theoretical guarantees, they only apply to limited settings (e.g., binary groups and labels), so there is room to improve fairness in other settings.

We also verify that, in the above setting, the identity matrix approximation indeed gets almost the same group ratios with the *exact inverse Hessian* computation. See more details in Sec. A.5.

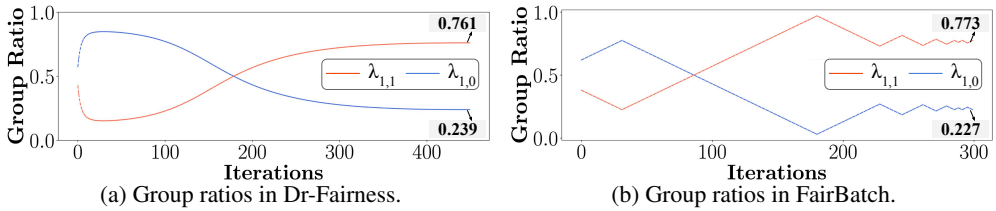

(a) Group ratios in Dr-Fairness. (b) Group ratios in FairBatch.

Figure 2: Comparison of group ratios $\boldsymbol{\lambda}$ from Dr-Fairness and FairBatch. Both converge to similar ratios.

3 Experiments

We perform various experiments to evaluate our algorithm. We repeat all experiments with three random seeds and measure all performances on a separate test set – see more information, including hyperparameter details of the algorithms, in Sec. B.1. We use ResNet50 (He et al., 2016) and the Adam optimizer (Kingma & Ba, 2015) – see results on ViT (Dosovitskiy et al., 2021) in Sec. B.9.

Datasets We utilize two real-world datasets: 1) CelebA (Liu et al., 2015) to compare our algorithms with baselines and perform various analyses, and 2) ImageNet People Subtree (Yang et al., 2020) to further observe the algorithm performances on a large-scale real-world scenario. Note that we are using large datasets instead of the traditional smaller tabular benchmarks for fairness because our goal is to make Dr-Fairness work in large-scale real-world applications.

[*CelebA*] Contains celebrity images, where each image has 40 attributes (e.g., gender, age, and smiling). We choose group and label attributes that are less subjective and traditionally considered for fairness. The group attributes are `gender` (male and female) and `age` (young and old). The label attributes are `age`, `haircolor` (black, blond, and others), and `smiling` (smiling and not-smiling).

Note that `age` can be used as either the group or label attribute. The sizes of the training, validation, and test sets are 160k, 20k, and 20k, respectively.

[*ImageNet People Subtree*] Contains 284 label classes and 3 group attributes: `gender` (male, female, and unsure), `skin color` (light, medium, and dark), and `age` (child, adult, middle, and retired). We first filter out classes that are vague, duplicates, or too small with few samples, which leaves us with 112 classes – see details in Sec. B.2. These classes contain about 111k samples, but only 10% of them have group attribute annotations. We split the group-labeled data into 40%, 20%, and 40% for training, validation, and testing, respectively.

Data generation We create the generated datasets using state-of-the-art generative models that conditionally synthesize images for each (y, z)-class. For CelebA, we use a StyleGAN-based controllable generation method called LACE (Nie et al., 2021). For ImageNet People Subtree, we fine-tune a diffusion model (Dhariwal & Nichol, 2021) pre-trained on ImageNet (Deng et al., 2009), and use classifier guidance (Song et al., 2020; Dhariwal & Nichol, 2021) to sample images in each (y, z)-class. Note that the controllable generation for ImageNet People Subtree is more challenging due to its large number of (y, z)-classes and labeling noises. Thus, the resulting generated data has lower quality than the generated data in CelebA. More details on data generation are in Sec. B.3.

Baselines We compare our algorithm with three types of baselines: 1) vanilla (non-fair) baseline, 2) fair pre-processing baselines, and 3) fair in-processing baselines.

For fair pre-processing training, we consider three baselines: *simple sampling*, *pair-augmenting (PairAug)* (Ramaswamy et al., 2021), and *pair-augmenting with our generated data (PairAug*)*. For simple sampling, we over- and under-sample the real data to ensure an equal ratio among groups. PairAug is a fair augmentation technique that uses the generation methods to synthesize balanced images for groups to reduce the correlation between the group and label attributes. For a fair comparison, we also implement an extension of PairAug (denoted by PairAug*), which uses the same balancing ratio in Ramaswamy et al. (2021), but uses our generated data.

For fair in-processing training, we consider three baselines: *fairness constraint* (Zafar et al., 2017a;b), *domain independence* (Wang et al., 2020), and *FairBatch* (Roh et al., 2021). Fairness constraint adds a fairness penalty term to the loss function to reduce the unfairness. Domain independence trains separate classifiers per each group to reduce the correlation between the group and label attributes. At inference, one can ensemble the outputs of the trained classifiers to get the final predictions. FairBatch adaptively adjusts batch ratios among groups to improve fairness only using real data.

Metrics We focus on two accuracy metrics and three fairness metrics. [*Accuracy*] We measure the standard accuracy over all samples and the balanced accuracy that averages y-class-wise accuracies. [*Fairness*] We focus on equalized odds (EO) (Hardt et al., 2016), demographic parity (DP) (Feldman et al., 2015), and bias amplification (Zhao et al., 2017). For EO and DP, we measure the disparities (i.e., unfairness) among groups: *EO disp.* $= \max_{z\in\mathbb{Z},y\in\mathbb{Y}} |\Pr(\hat{\mathrm{y}}{=}y|\mathrm{z}{=}z,\mathrm{y}{=}y) - \Pr(\hat{\mathrm{y}}{=}y|\mathrm{y}{=}y)|$, and *DP disp.*$= \max_{z\in\mathbb{Z}} |\Pr(\hat{\mathrm{y}}{=}1|\mathrm{z}{=}z) - \Pr(\hat{\mathrm{y}}{=}1)|$. Together with either EO or DP, we measure bias amplification to see how much the data bias is amplified in the model: *Bias amp.* $= \max_{y\in\mathbb{Y}} \Pr(\mathrm{z}{=}z|\hat{\mathrm{y}}{=}y) - \Pr(\mathrm{z}{=}z|\mathrm{y}{=}y)$, where $z := \arg\max_{z'\in\mathbb{Z}} \Pr(\mathrm{z}{=}z'|\hat{\mathrm{y}}{=}y)$. Here, a good performance is indicated by high accuracy values and low EO disp., DP disp., and bias amp. values.

3.1 CelebA Experiments

We evaluate Dr-Fairness on CelebA by comparing it with baselines (Sec. 3.1.1) and analyzing the impact of its hyperparameters (Sec. 3.1.2), components (Sec. 3.1.3), and generated data (Sec. 3.1.4).

3.1.1 Accuracy and Fairness

Table 2 shows the accuracy and fairness performances of different algorithms on CelebA when training w.r.t. EO (see results of training w.r.t. DP in Sec. B.5). Here we consider two scenarios: 1) binary setting of y (age) & z (gender) and 2) non-binary setting of y (haircolor) & z (gender, age). In Sec. B.6, we show similar results for the experiments on other group and label combinations. Also, in Sec. B.7, we visually demonstrate the accuracy-fairness tradeoffs of the algorithms.

The fair pre-processing baselines (in rows 2–4) improve the fairness performances compared to the original non-fair baseline, but still perform worse (i.e., lower EO disp. and lower bias amp.) than the fair in-processing baselines and Dr-Fairness. Thus, simply equalizing the data ratio among groups may not be enough to achieve high group fairness. Note that it is not straightforward to get the

Table 2: Performances on the CelebA test set when training w.r.t. EO on two scenarios: binary y (age) & z (gender) and non-binary y (haircolor) & z (gender, age). We compare Dr-Fairness with three types of baselines: 1) non-fair baseline, 2) fair pre-processing baselines: Simple Sampling, PairAug, and PairAug*, and 3) fair in-processing baselines: Fair. Const., Dom. Indep., and FairBatch. Note that PairAug and Fair. Const. cannot be trivially extended to the non-binary label setting, so we only show their results in the first column.

	y: age and z: gender				y: haircolor and z: (gender, age)			
Method	Acc.	Bal. Acc.	EO Disp.	Bias Amp.	Acc.	Bal. Acc.	EO Disp.	Bias Amp.
Non-fair	86.4±0.3	76.4±0.2	0.173±0.023	0.101±0.022	83.8±0.3	82.0±0.6	0.535±0.049	0.014±0.003
Simple Sampling	86.8±0.2	78.3±0.5	0.132±0.019	0.052±0.017	83.2±0.4	80.9±0.3	0.421±0.016	0.026±0.002
PairAug (Ramaswamy et al., 2021)	85.6±0.6	79.8±0.3	0.124±0.002	0.030±0.003	-	-	-	-
PairAug* (Ramaswamy et al., 2021)	86.7±0.2	79.3±0.6	0.134±0.008	0.053±0.008	83.0±0.2	80.1±0.8	0.406±0.026	0.022±0.005
Fair. Const. (Zafar et al., 2017b)	86.8±0.2	79.6±0.5	0.106±0.014	0.028±0.012	-	-	-	-
Dom. Indep. (Wang et al., 2020)	85.0±0.7	72.4±2.1	0.070±0.008	0.034±0.021	81.7±0.6	74.8±1.4	0.340±0.041	0.026±0.013
FairBatch (Roh et al., 2021)	84.7±0.3	72.5±1.8	0.023±0.014	**-0.043±0.007**	79.4±1.5	68.2±4.7	0.096±0.033	0.033±0.003
Dr-Fairness	**87.7±0.3**	**81.0±0.2**	**0.020±0.010**	-0.026±0.002	**85.0±0.1**	**84.4±0.3**	**0.079±0.023**	**0.012±0.002**

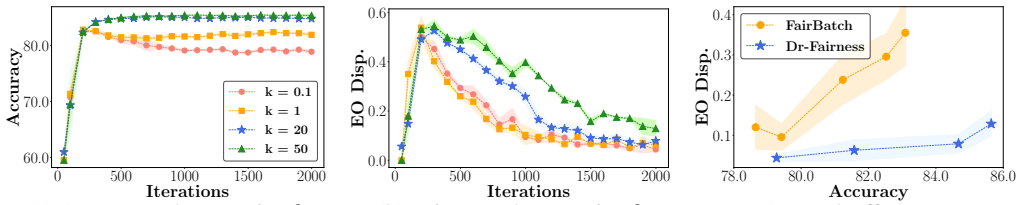

(a) Accuracy when varying k. (b) Fairness when varying k. (c) Tradeoff curves.

Figure 3: The performances of Dr-Fairness by varying the hyperparameter k when (y, z) = (haircolor, (gender, age)). The first two graphs show the performance changes during the training, and the last graph shows the accuracy-fairness tradeoff curves. Compared to FairBatch, Dr-Fairness shows a better tradeoff.

generated data from the original PairAug work in the non-binary label setting, so we are not able to report the numbers (e.g., the right columns of Table 2). But we expect that the results would be similar to PairAug*, as observed in the binary setting. Additionally, FairnessGAN (Sattigeri et al., 2019) is another previous method that aims to generate fair images, but this method has been reported to show worse fairness and accuracy performances than PairAug – see Sec. B.4 for a detailed comparison.

The fair in-processing baselines (in rows 5–7) improve fairness (esp. EO), but tend to sacrifice accuracy because they only utilize real data. Here, in the baselines with higher fairness, the decrease in accuracy becomes more significant. For example, FairBatch adaptively adjusts the group ratio on real data to improve fairness, but we observe that some small-sized groups end up being oversampled, which is detrimental to the accuracy performance on the test set.

In comparison, Dr-Fairness achieves high fairness performances while even improving accuracies by adaptively finding optimal data ratios among groups and between real and generated data. There are two takeaways: 1) we can find a better group ratio than the 1:1 ratio for fairness, and 2) an optimal combination of real and generated data can mitigate the accuracy degradation of fair training.

3.1.2 Hyperparameter Analysis

We now evaluate Dr-Fairness by varying its main hyperparameter k used in the bilevel optimization. A larger k puts more weight on the accuracy loss than the fairness loss. Figures 3a and 3b show the accuracy and fairness of Dr-Fairness during the training with the different k values. As expected, increasing k (say k = 50) results in higher accuracy and lower fairness. By varying k, we can also compare the accuracy-fairness tradeoff curves of Dr-Fairness and FairBatch in Figure 3c. Dr-Fairness shows a better tradeoff, which is consistent with the results in Sec. 3.1.1.

3.1.3 Ablation Study

We perform an ablation study on our framework to evaluate the impact of each component in the optimization on fairness and accuracy. For fairness, we conduct two ablations: F1) remove both the fairness loss in the outer objective and $\lambda_{y,z}$ in the inner objective, and F2) only remove the fairness loss in the outer objective. For accuracy, we consider three ablations: A1) remove the accuracy loss in the outer objective; and $\mu_{y,z}$ and the generated data loss in the inner objective, A2) remove $\mu_{y,z}$ and the generated data loss in the inner objective, and A3) only remove the accuracy loss in the outer objective. We note that A2 also represents how Dr-Fairness works only with real data when we

cannot utilize generated data. Through this sequence of ablations, we observe that each part of our algorithm gradually improves the fairness and accuracy performances.

In Table 3, the fairness ablations (in rows 1–2) show worse fairness as the fairness loss and $\lambda_{y,z}$ are discarded, and the accuracy ablations (in rows 3–5) demonstrate lower accuracy and balanced accuracy as some of the accuracy loss, generated data, and $\mu_{y,z}$ are removed. We thus conclude that all components in our bilevel optimization contribute to the overall performances.

Table 3: Ablation study on CelebA, where we consider the setting of non-binary y (haircolor) and binary z (gender). We mark noticeable *performance degradations* with underlines.

Method	Acc.	Bal. Acc.	EO Disp.
F1: w/o fair. loss and $\lambda_{y,z}$	$85.7_{\pm 0.3}$	$83.9_{\pm 1.0}$	$\underline{0.432_{\pm 0.063}}$
F2: w/o fair. loss	$85.1_{\pm 0.3}$	$84.6_{\pm 0.3}$	$\underline{0.261_{\pm 0.017}}$
A1: w/o acc. loss, $\mu_{y,z}$, and gen. data	$\underline{79.3_{\pm 1.2}}$	$\underline{66.7_{\pm 3.8}}$	$0.090_{\pm 0.058}$
A2: w/o $\mu_{y,z}$, and gen. data	$\underline{80.0_{\pm 1.2}}$	$\underline{70.8_{\pm 3.1}}$	$0.031_{\pm 0.012}$
A3: w/o acc. loss	$\underline{71.5_{\pm 0.9}}$	$82.1_{\pm 0.8}$	$0.046_{\pm 0.029}$
Dr-Fairness	$84.5_{\pm 0.2}$	$82.3_{\pm 0.7}$	$0.029_{\pm 0.009}$

3.1.4 Generated Data of Different Qualities

We analyze the robustness of our framework against the generated data quality as shown in Table 4. We vary the quality of generated data by adding random Gaussian noise to the original images. Interestingly, when the generated data quality decreases (i.e., adding more noise to the images), Dr-Fairness automatically reduces the usage of the generated data, as shown in the second column of Table 4. With this automatic adjustment, Dr-Fairness shows robust performances in the last three columns. When the generated data is fully replaced with Gaussian noise (i.e., severe noise), the accuracy and fairness performances become worse than the clean setting as expected, but the fairness score is still much better than the non-fair baseline by reasonably sacrificing the accuracy. These results show that Dr-Fairness is effective even with low-quality generated data.

Table 4: Analysis of the behavior of Dr-Fairness when the quality of generated data changes. We add different amounts of Gaussian noise to the original (clean) generated data. In the severe case, we fully replace the generated data with the noise. We set y to haircolor (non-binary) and z to gender (binary).

Noise level in gen. data	Final gen. data ratio found in Dr-Fairness	Acc.	Bal. Acc.	EO Disp.
Clean	$0.224_{\pm 0.009}$	$84.5_{\pm 0.2}$	$82.3_{\pm 0.7}$	$0.029_{\pm 0.009}$
Light noise	$0.210_{\pm 0.018}$	$84.4_{\pm 0.2}$	$81.6_{\pm 1.0}$	$0.033_{\pm 0.003}$
Mid noise	$0.192_{\pm 0.012}$	$84.5_{\pm 0.1}$	$81.9_{\pm 0.3}$	$0.039_{\pm 0.022}$
Severe noise	$0.114_{\pm 0.041}$	$83.1_{\pm 1.8}$	$78.3_{\pm 0.8}$	$0.108_{\pm 0.038}$
Non-fair baseline	–	$83.8_{\pm 0.3}$	$82.0_{\pm 0.6}$	$0.399_{\pm 0.019}$

3.2 ImageNet People Subtree Experiments

We finally perform experiments on ImageNet People Subtree, which represents a large-scale real-world scenario. As only 10% of the data has group annotations, following Zhao et al. (2021), we first pre-train a non-fair model on the entire training set with y labels and then fine-tune the pre-trained model to improve fairness on the small set with group labels.

Tables 5 (below) and 10 (in Sec. B.8) show the performances of the algorithms on four group scenarios: gender, skin color, age, and all combinations of them. The overall results are consistent with the CelebA experiments, where we can see Dr-Fairness outperforms the baselines in accuracy, fairness, or both. Specifically, our algorithm shows the best or second-best performance on EO disparity and bias amplification in almost all group settings while obtaining better classification accuracies compared to the baselines with similar fairness scores. For example, we obtain classification accuracies better than FairBatch, with an absolute improvement of 5–9%, while achieving similar fairness scores.

As ImageNet People Subtree shows a more complicated real-world scenario than CelebA, we have two additional observations. First, when we train the baselines w.r.t. EO, the bias amplification metric occasionally gets worse compared to the original model (e.g., Dom. Indep. on gender and FairBatch on skin color). This result shows that improving EO, which aims to minimize the label-specific accuracy gap between groups, does not necessarily lead to reducing the bias in the model compared to the data. In addition, as domain independence trains separate classifiers per each group, we suspect that the final model may have undesirable results (e.g., worse bias amp.) if some of the classifiers fail. Second, this dataset contains a large number of (y, z)-classes where many of them are extremely small-sized. Here the controllable data generation becomes challenging where the generated labels may be noisy, which negatively affects the fair training as well. Nonetheless, Dr-Fairness still shows a clear improvement in fairness compared to the baselines, and we believe more data with clean labels could further improve its performance.

The above experiments use ResNet50 (He et al., 2016) as the model backbone. In Sec. B.9, we also conduct experiments using ViT (Dosovitskiy et al., 2021) and observe similar results. The results imply our method is applicable to different network architectures.

Table 5: Performances on the ImageNet People Subtree test set when training w.r.t. equalized odds (EO) for either age or all combinations of groups. Other settings are identical to Table 2.

	z: age				z: (gender, skin color, age)			
Method	Acc.	Bal. Acc.	EO Disp.	Bias Amp.	Acc.	Bal. Acc.	EO Disp.	Bias Amp.
Non-fair	61.4±0.8	61.8±0.8	0.849±0.029	0.191±0.039	61.4±0.8	61.8±0.8	0.918±0.016	0.270±0.107
Simple Sampling	53.4±0.9	53.6±0.9	0.822±0.044	0.201±0.077	54.6±0.9	54.8±0.8	0.885±0.041	0.181±0.002
PairAug* (Ramaswamy et al., 2021)	55.6±1.2	55.9±1.3	0.820±0.046	0.168±0.022	57.6±0.4	57.9±0.5	0.871±0.005	0.153±0.036
Dom. Indep. (Wang et al., 2020)	**59.9±0.2**	**60.1±0.3**	0.838±0.019	0.220±0.006	50.0±0.9	50.1±0.9	0.897±0.015	0.254±0.020
FairBatch (Roh et al., 2021)	51.3±1.2	51.5±1.2	0.798±0.042	0.198±0.003	50.1±5.3	50.3±5.3	**0.853±0.013**	0.185±0.021
Dr-Fairness	59.7±0.1	59.9±0.1	**0.784±0.011**	**0.149±0.012**	**58.7±0.5**	**59.1±0.5**	0.866±0.012	**0.146±0.006**

4 Related Work

As model fairness becomes indispensable for Trustworthy AI, numerous works have been recently proposed to better measure fairness and design fairness-aware algorithms (Narayanan, 2018). Among various fairness definitions, we focus on group fairness measures (Hardt et al., 2016; Feldman et al., 2015), which are widely studied in the fairness literature – see representative works in Sec. C. Unfortunately most of the existing algorithms are not designed to handle large number of groups or labels, and our contribution is to support such large-scale scenarios for real-world applications.

Among the previous techniques, FairBatch (Roh et al., 2021) is the most relevant to our work as it finds the optimal group ratio for fairness on real data and shows the state-of-the-art fairness performances on various tabular datasets, including COMPAS (Angwin et al., 2016) and AdultIncome (Kohavi, 1996). However, FairBatch may suffer from accuracy degradation due to oversampling on very small-size groups, especially in vision datasets. In particular, FairBatch cannot utilize accuracy-based objectives and generated data, which may result in a worse accuracy and fairness tradeoff. Also, the theoretical guarantees of FairBatch do not apply in our setting because the outer objective of our bilevel optimization problem is non-convex. In contrast, Dr-Fairness can minimize the accuracy degradation of fair training by optimally utilizing both real and generated data based on the fairness and accuracy objectives.

There is an emerging line of research for fairness in visual recognition (Najibi, 2020; Wang et al., 2020) where using generated data is critical. Many visual recognition tasks involve multiple classes of varying sizes, and only using real data is often insufficient to improve fairness. In response, several works have proposed new algorithms to create a balanced dataset by augmenting the biased real dataset with well-controlled generated data (Sattigeri et al., 2019; Choi et al., 2020; Ramaswamy et al., 2021). However, simply balancing the data sizes is not enough to achieve high-enough group fairness, as the learning difficulty and generated data quality can differ across groups. Although a recent work (Zietlow et al., 2022) suggests an adaptive data augmentation that generating more data for worse-performing groups, it uses heuristics to adjust data ratios without proper optimization and thus has limited fairness performance. In comparison, Dr-Fairness solves a novel bilevel optimization problem to find optimal data ratios and thus obtains both high fairness and accuracy.

In addition, there are other related studies on fair data reweighing (Li & Liu, 2022; Jiang & Nachum, 2020; Krasanakis et al., 2018), fair augmentation (Chuang & Mroueh, 2021), and fair representations (Shui et al., 2022). Compared to our work, these studies only use real data or do not scale to large datasets – see a detailed discussion in Sec. C.

5 Conclusion

We proposed a novel adaptive sampling approach called Dr-Fairness that utilizes both real and generated data for fairness. To perform adaptive sampling systematically, we first formulated a bilevel optimization, where the goal is to find the optimal data ratios among sensitive groups and between real and generated data to achieve high group fairness while minimizing accuracy degradation. To solve the bilevel optimization problem, we then designed an efficient approximate algorithm based on the implicit function theorem and identity-matrix approximation. Extensive experiments on the CelebA and ImageNet People Subtree datasets showed that Dr-Fairness achieves state-of-the-art fairness and accuracy performances. We believe Dr-Fairness opens up new opportunities for effectively using generated data in large-scale real-world scenarios.

ETHICS STATEMENT

We believe our work can positively impact society by reducing discrimination in AI applications. In particular, our framework shows that generated data can compensate for unfairness issues in real data (e.g., size bias and lack of diversity) to help obtain better accuracy and fairness results that would not have been possible otherwise. As a result, real-world applications have a better chance of ensuring fairness without sacrificing accuracy unnecessarily.

We do note that choosing an appropriate fairness metric for each application is essential, as a poor choice may lead to unintended discrimination. Thus, one needs to carefully choose the target fairness metrics based on the social context in each application. Also, in terms of privacy, we did not involve human subjects or use any direct personal identifiers in the experiments, except for the human images in the publicly available benchmark datasets.

REPRODUCIBILITY STATEMENT

We provide implementation and experimental details (e.g., libraries, hyperparameters, data preprocessing, and data generation) in Sec. 3 and Sec. B to enable the reproduction of our results. To help with the reproducibility of results in this paper, we will make our source code publicly available in the future.

REFERENCES

Alekh Agarwal, Alina Beygelzimer, Miroslav Dudík, John Langford, and Hanna M. Wallach. A reductions approach to fair classification. In *ICML*, pp. 60–69, 2018.

Julia Angwin, Jeff Larson, Surya Mattu, and Lauren Kirchner. Machine bias: There's software used across the country to predict future criminals. And its biased against blacks. ProPublica, 2016.

L. Elisa Celis, Lingxiao Huang, Vijay Keswani, and Nisheeth K. Vishnoi. Fair classification with noisy protected attributes: A framework with provable guarantees. In *ICML*, 2021.

Kristy Choi, Aditya Grover, Trisha Singh, Rui Shu, and Stefano Ermon. Fair generative modeling via weak supervision. In *ICML*, 2020.

Ching-Yao Chuang and Youssef Mroueh. Fair mixup: Fairness via interpolation. *ICLR*, 2021.

Oswaldo de Oliveira. The implicit and the inverse function theorems: easy proofs. *Real Analysis Exchange*, 39(1):207–218, 2014.

Jia Deng, Wei Dong, Richard Socher, Li-Jia Li, Kai Li, and Li Fei-Fei. Imagenet: A large-scale hierarchical image database. In *2009 IEEE conference on computer vision and pattern recognition*, pp. 248–255. Ieee, 2009.

Prafulla Dhariwal and Alexander Nichol. Diffusion models beat gans on image synthesis. *NeurIPS*, 34:8780–8794, 2021.

Alexey Dosovitskiy, Lucas Beyer, Alexander Kolesnikov, Dirk Weissenborn, Xiaohua Zhai, Thomas Unterthiner, Mostafa Dehghani, Matthias Minderer, Georg Heigold, Sylvain Gelly, Jakob Uszkoreit, and Neil Houlsby. An image is worth 16x16 words: Transformers for image recognition at scale. In *ICLR*, 2021.

Cynthia Dwork, Moritz Hardt, Toniann Pitassi, Omer Reingold, and Richard S. Zemel. Fairness through awareness. In *ITCS*, pp. 214–226, 2012.

Michael Feldman, Sorelle A. Friedler, John Moeller, Carlos Scheidegger, and Suresh Venkatasubramanian. Certifying and removing disparate impact. In *SIGKDD*, pp. 259–268, 2015.

Chelsea Finn, Pieter Abbeel, and Sergey Levine. Model-agnostic meta-learning for fast adaptation of deep networks. In *ICML*, pp. 1126–1135. PMLR, 2017.

Samy Wu Fung, Howard Heaton, Qiuwei Li, Daniel McKenzie, Stanley Osher, and Wotao Yin. Jfb: Jacobian-free backpropagation for implicit networks. In *AAAI*, 2022.

Zhengyang Geng, Meng-Hao Guo, Hongxu Chen, Xia Li, Ke Wei, and Zhouchen Lin. Is attention better than matrix decomposition? In *ICLR*, 2021.

Moritz Hardt, Eric Price, and Nati Srebro. Equality of opportunity in supervised learning. In *NeurIPS*, pp. 3315–3323, 2016.

Tatsunori Hashimoto, Megha Srivastava, Hongseok Namkoong, and Percy Liang. Fairness without demographics in repeated loss minimization. In *ICML*, pp. 1929–1938, 2018.

Kaiming He, Xiangyu Zhang, Shaoqing Ren, and Jian Sun. Deep residual learning for image recognition. In *CVPR*, pp. 770–778, 2016.

Heinrich Jiang and Ofir Nachum. Identifying and correcting label bias in machine learning. In *AISTATS*, pp. 702–712, 2020.

Faisal Kamiran and Toon Calders. Data preprocessing techniques for classification without discrimination. *Knowl. Inf. Syst.*, 33(1):1–33, 2011.

Tero Karras, Samuli Laine, Miika Aittala, Janne Hellsten, Jaakko Lehtinen, and Timo Aila. Analyzing and improving the image quality of stylegan. In *IEEE CVPR*, pp. 8110–8119, 2020.

Diederik P. Kingma and Jimmy Ba. Adam: A method for stochastic optimization. In Yoshua Bengio and Yann LeCun (eds.), *ICLR*, 2015.

Ron Kohavi. Scaling up the accuracy of naive-bayes classifiers: A decision-tree hybrid. In *SIGKDD*, pp. 202–207, 1996.

Steven George Krantz and Harold R Parks. *The implicit function theorem: history, theory, and applications*. Springer Science & Business Media, 2002.

Emmanouil Krasanakis, Eleftherios Spyromitros-Xioufis, Symeon Papadopoulos, and Yiannis Kompatsiaris. Adaptive sensitive reweighting to mitigate bias in fairness-aware classification. In *WWW*, pp. 853–862, 2018.

Matt J Kusner, Joshua Loftus, Chris Russell, and Ricardo Silva. Counterfactual fairness. In *NeurIPS*, pp. 4066–4076. 2017.

Peizhao Li and Hongfu Liu. Achieving fairness at no utility cost via data reweighing. *ICML*, 2022.

Hanxiao Liu, Karen Simonyan, and Yiming Yang. Darts: Differentiable architecture search. In *ICLR*, 2018.

Risheng Liu, Jiaxin Gao, Jin Zhang, Deyu Meng, and Zhouchen Lin. Investigating bi-level optimization for learning and vision from a unified perspective: A survey and beyond. *IEEE TPAMI*, 2021.

Ziwei Liu, Ping Luo, Xiaogang Wang, and Xiaoou Tang. Deep learning face attributes in the wild. In *IEEE ICCV*, pp. 3730–3738, 2015.

Jonathan Lorraine, Paul Vicol, and David Duvenaud. Optimizing millions of hyperparameters by implicit differentiation. In *AISTATS*, pp. 1540–1552. PMLR, 2020.

Jelena Luketina, Mathias Berglund, Klaus Greff, and Tapani Raiko. Scalable gradient-based tuning of continuous regularization hyperparameters. In *ICML*, pp. 2952–2960. PMLR, 2016.

Dougal Maclaurin, David Duvenaud, and Ryan Adams. Gradient-based hyperparameter optimization through reversible learning. In *ICML*, pp. 2113–2122. PMLR, 2015.

Sébastien Marcel and Yann Rodriguez. Torchvision the machine-vision package of torch. In *ACM ICM*, pp. 1485–1488, 2010.

Ninareh Mehrabi, Fred Morstatter, Nripsuta Saxena, Kristina Lerman, and Aram Galstyan. A survey on bias and fairness in machine learning. *ACM Computing Surveys*, 54(6):1–35, 2021.

Aditya Krishna Menon and Robert C Williamson. The cost of fairness in binary classification. In *FAT**, pp. 107–118, 2018.

Alex Najibi. Racial discrimination in face recognition technology. *Harvard Online: Science Policy and Social Justice*, 24, 2020.

Arvind Narayanan. Translation tutorial: 21 fairness definitions and their politics. In *ACM FAccT*, volume 1170, 2018.

Weili Nie, Arash Vahdat, and Anima Anandkumar. Controllable and compositional generation with latent-space energy-based models. *NeurIPS*, 34:13497–13510, 2021.

OpenAI. Dall·e 2. `https://openai.com/dall-e-2/`, 2022.

Adam Paszke, Sam Gross, Soumith Chintala, Gregory Chanan, Edward Yang, Zachary DeVito, Zeming Lin, Alban Desmaison, Luca Antiga, and Adam Lerer. Automatic differentiation in PyTorch. In *NIPS Autodiff Workshop*, 2017.

Fabian Pedregosa. Hyperparameter optimization with approximate gradient. In *ICML*, pp. 737–746. PMLR, 2016.

Tapani Raiko, Harri Valpola, and Yann LeCun. Deep learning made easier by linear transformations in perceptrons. In *Artificial intelligence and statistics*, pp. 924–932. PMLR, 2012.

Aravind Rajeswaran, Chelsea Finn, Sham M Kakade, and Sergey Levine. Meta-learning with implicit gradients. *Advances in neural information processing systems*, 32, 2019.

Vikram V Ramaswamy, Sunnie SY Kim, and Olga Russakovsky. Fair attribute classification through latent space de-biasing. In *IEEE CVPR*, pp. 9301–9310, 2021.

Yuji Roh, Kangwook Lee, Steven Euijong Whang, and Changho Suh. FR-Train: A mutual information-based approach to fair and robust training. In *ICML*, pp. 8147–8157, 2020.

Yuji Roh, Kangwook Lee, Steven Euijong Whang, and Changho Suh. FairBatch: Batch selection for model fairness. In *ICLR*, 2021.

Robin Rombach, Andreas Blattmann, Dominik Lorenz, Patrick Esser, and Björn Ommer. Stable diffusion. `https://github.com/CompVis/stable-diffusion`, 2022.

Prasanna Sattigeri, Samuel C Hoffman, Vijil Chenthamarakshan, and Kush R Varshney. Fairness gan: Generating datasets with fairness properties using a generative adversarial network. *IBM Journal of Research and Development*, 63(4/5):3–1, 2019.

Aili Shen, Xudong Han, Trevor Cohn, Timothy Baldwin, and Lea Frermann. Optimising equal opportunity fairness in model training. *ACL*, 2022.

Changjian Shui, Qi Chen, Jiaqi Li, Boyu Wang, and Christian Gagné. Fair representation learning through implicit path alignment. *ICML*, 2022.

Yang Song, Jascha Sohl-Dickstein, Diederik P Kingma, Abhishek Kumar, Stefano Ermon, and Ben Poole. Score-based generative modeling through stochastic differential equations. *arXiv preprint arXiv:2011.13456*, 2020.

Hugo Touvron, Matthieu Cord, Matthijs Douze, Francisco Massa, Alexandre Sablayrolles, and Herve Jegou. Training data-efficient image transformers & distillation through attention. In *International Conference on Machine Learning*, 2021.

Zeyu Wang, Klint Qinami, Ioannis Christos Karakozis, Kyle Genova, Prem Nair, Kenji Hata, and Olga Russakovsky. Towards fairness in visual recognition: Effective strategies for bias mitigation. In *IEEE CVPR*, pp. 8919–8928, 2020.

Bryan Wilder, Eric Ewing, Bistra Dilkina, and Milind Tambe. End to end learning and optimization on graphs. *NeurIPS*, 32, 2019.

Kaiyu Yang, Klint Qinami, Li Fei-Fei, Jia Deng, and Olga Russakovsky. Towards fairer datasets: Filtering and balancing the distribution of the people subtree in the imagenet hierarchy. In *FAT**, pp. 547–558, 2020.

Muhammad Bilal Zafar, Isabel Valera, Manuel Gomez-Rodriguez, and Krishna P. Gummadi. Fairness constraints: Mechanisms for fair classification. In *AISTATS*, pp. 962–970, 2017a.

Muhammad Bilal Zafar, Isabel Valera, Manuel Gomez-Rodriguez, and Krishna P. Gummadi. Fairness beyond disparate treatment & disparate impact: Learning classification without disparate mistreatment. In *WWW*, pp. 1171–1180, 2017b.

Richard S. Zemel, Yu Wu, Kevin Swersky, Toniann Pitassi, and Cynthia Dwork. Learning fair representations. In *ICML*, pp. 325–333, 2013.

Brian Hu Zhang, Blake Lemoine, and Margaret Mitchell. Mitigating unwanted biases with adversarial learning. In *AIES*, pp. 335–340, 2018a.

Hongyi Zhang, Moustapha Cisse, Yann N Dauphin, and David Lopez-Paz. mixup: Beyond empirical risk minimization. *ICLR*, 2018b.

Eric Zhao, De-An Huang, Hao Liu, Zhiding Yu, Anqi Liu, Olga Russakovsky, and Anima Anandkumar. Scaling fair learning to hundreds of intersectional groups. 2021.

Jieyu Zhao, Tianlu Wang, Mark Yatskar, Vicente Ordonez, and Kai-Wei Chang. Men also like shopping: Reducing gender bias amplification using corpus-level constraints. In *EMNLP*, pp. 2979–2989, 2017.

Dominik Zietlow, Michael Lohaus, Guha Balakrishnan, Matthäus Kleindessner, Francesco Locatello, Bernhard Schölkopf, and Chris Russell. Leveling down in computer vision: Pareto inefficiencies in fair deep classifiers. In *IEEE CVPR*, pp. 10410–10421, 2022.

A Appendix – Optimization and Algorithm

A.1 Bilevel Optimization for Demographic Parity

Continuing from Sec. 2.1, we formulate our bilevel optimization w.r.t. demographic parity (DP) as follows:

$$\min_{\boldsymbol{\lambda},\boldsymbol{\mu}} \max_{y\in\mathbb{Y},z_1,z_2\in\mathbb{Z}} \{|\tfrac{m_{y,z_1}}{m_{\star,z_1}} L^{\text{real}}_{y,z_1}(\boldsymbol{w}(\boldsymbol{\lambda},\boldsymbol{\mu})) - \tfrac{m_{y,z_2}}{m_{\star,z_2}} L^{\text{real}}_{y,z_2}(\boldsymbol{w}(\boldsymbol{\lambda},\boldsymbol{\mu}))|\} + k \sum_{y\in\mathbb{Y},z\in\mathbb{Z}} \tfrac{m_{y,z}}{m} L^{\text{real}}_{y,z}(\boldsymbol{w}(\boldsymbol{\lambda},\boldsymbol{\mu})),$$

$$\boldsymbol{w}(\boldsymbol{\lambda},\boldsymbol{\mu}) = \arg\min_{\boldsymbol{w}} \sum_{y\in\mathbb{Y},z\in\mathbb{Z}} \frac{m_{y,\star}}{m} \lambda_{y,z}\{\mu_{y,z} L^{\text{real}}_{y,z}(\boldsymbol{w}) + (1-\mu_{y,z}) L^{\text{gen}}_{y,z}(\boldsymbol{w})\},$$

$$\text{s.t.} \quad \boldsymbol{\lambda}\in[0,1], \boldsymbol{\mu}\in[0,1], \ \textstyle\sum_{z\in\mathbb{Z}} \lambda_{y,z} = 1, \forall y\in\mathbb{Y},$$

where $\mathbb{Y} = \{0,1\}$. Note that DP is designed for binary classification. For designing the fairness loss, we are inspired by Roh et al. (2021), which gives a hint on formulating DP loss in bilevel optimization. Intuitively, the fractions in the fairness loss make the model reduces the disparity of each prediction ratio across groups, without considering the sizes of true label classes. This strategy can be a sufficient condition for DP, as the goal of DP is to achieve the same positive prediction ratio among groups – see more details in Roh et al. (2021).

A.2 Capturing Equalized Odds with the Loss Constraint

Continuing from Sec. 2.1, we explain how the loss-based constraints can capture equalized odds. We recall our notation: the empirical risk over samples in the set $(\mathrm{y}=y, \mathrm{z}=z)$ is $L_{y,z}(\boldsymbol{w}) := \frac{1}{m_{y,z}} \sum_{i:\mathrm{y}_i=y,\mathrm{z}_i=z} \ell(\mathrm{y}_i, \hat{\mathrm{y}}_i)$, where $\ell(\mathrm{y}_i, \hat{\mathrm{y}}_i)$ is the loss function. Here, when the loss function $\ell(\mathrm{y}_i, \hat{\mathrm{y}}_i)$ is 1/0-loss (i.e., $\ell(\mathrm{y}_i, \hat{\mathrm{y}}_i) = 1(\mathrm{y}_i \neq \hat{\mathrm{y}}_i)$, where $1(\cdot)$ is an indicator function), the loss-based constraint can perfectly express the equalized odds disparity. Specifically, $L_{y,z}(\boldsymbol{w})$ with 1/0-loss is equivalent to the probability of the correct predictions in each (y, z)-class (i.e., $\Pr(\hat{\mathrm{y}}=y|\mathrm{y}=y, \mathrm{z}=z)$). Therefore, our fairness loss constraint (i.e., $\max_{y\in\mathbb{Y},z_1,z_2\in\mathbb{Z}}\{|L^{\text{real}}_{y,z_1}(\boldsymbol{w}(\boldsymbol{\lambda},\boldsymbol{\mu})) - L^{\text{real}}_{y,z_2}(\boldsymbol{w}(\boldsymbol{\lambda},\boldsymbol{\mu}))|\}$) becomes the equalized odds metric, which describes the class-conditioned accuracy disparity among groups (i.e., $\max_{y\in\mathbb{Y},z_1,z_2\in\mathbb{Z}} |\Pr(\hat{\mathrm{y}}=y|\mathrm{y}=y, \mathrm{z}=z_1) - \Pr(\hat{\mathrm{y}}=y|\mathrm{y}=y, \mathrm{z}=z_2)|$). In practice, we can also use other loss functions like cross-entropy loss instead of the 1/0-loss, as other loss functions have been empirically verified as reasonable proxies for capturing group fairness metrics (Roh et al., 2021; Shen et al., 2022).

A.3 Using the Implicit Function Theorem

Continuing from Sec. 2.2, we describe how we convert the best-response Jacobian in Eq. 1 using the implicit function theorem. We note that among various methods of solving bilevel optimization problems, the implicit function theorem significantly improves the algorithm efficiency with theoretical evidence. Here, we first state the original implicit function theorem:

Theorem 1. *(Implicit Function Theorem, stated in Krantz & Parks (2002); de Oliveira (2014)) Let $F: \mathbb{R}^n \times \mathbb{R}^m \to \mathbb{R}^m$ be a continuously differentiable function, where the input of F is $(\boldsymbol{x}, \boldsymbol{y}) \in \mathbb{R}^n \times \mathbb{R}^m$. Assume there is an input point $(\boldsymbol{a}, \boldsymbol{b})$ that satisfies $F(\boldsymbol{a}, \boldsymbol{b}) = \boldsymbol{0}$, and $\frac{\partial F(\boldsymbol{a},\boldsymbol{b})}{\partial \boldsymbol{y}}$ (i.e., the Jacobian matrix) is invertible. Then, there exist open sets $U \subset \mathbb{R}^n$ and $V \subset \mathbb{R}^m$ that contain $\boldsymbol{a}$ and $\boldsymbol{b}$, respectively, and satisfy the following:*

- *There is a unique continuously differentiable function G, where $G(\boldsymbol{a}) = \boldsymbol{b}$ and $F(\boldsymbol{x}, G(\boldsymbol{x})) = \boldsymbol{0}$ for all $\boldsymbol{x} \in U$.*
- *We have the Jacobian matrix of partial derivatives of G in U as follows:*

$$\frac{\partial G(\boldsymbol{x})}{\partial \boldsymbol{x}} = -[\frac{\partial F(\boldsymbol{x}, G(\boldsymbol{x}))}{\partial \boldsymbol{y}}]^{-1} [\frac{\partial F(\boldsymbol{x}, G(\boldsymbol{x}))}{\partial \boldsymbol{x}}].$$

We now apply the above theorem in our setting. To get the best-response Jacobian w.r.t. $\boldsymbol{\lambda}$, we consider $\frac{\partial f_{\text{inner}}(\boldsymbol{\lambda},\boldsymbol{w})}{\partial \boldsymbol{w}}$ as $F(\boldsymbol{x}, \boldsymbol{y})$ and $\boldsymbol{w}(\boldsymbol{\lambda})$ as $G(\boldsymbol{x})$. Note that when accessing the gradient w.r.t. $\boldsymbol{\lambda}$,

we can ignore $\boldsymbol{\mu}$ without loss of generality, and vice versa. Then, we can rewrite Theorem 1 for our scenario as follows:

Corollary 2. *(Implicit Function Theorem in our setting) Let* $\frac{\partial f_{inner}}{\partial \boldsymbol{w}} : \mathbb{R}^n \times \mathbb{R}^m \rightarrow \mathbb{R}^m$ *be a continuously differentiable function, where the input of* $\frac{\partial f_{inner}}{\partial \boldsymbol{w}}$ *is* $(\boldsymbol{\lambda}, \boldsymbol{w}) \in \mathbb{R}^n \times \mathbb{R}^m$*. Assume there is an input point* $(\boldsymbol{a}, \boldsymbol{b})$ *that satisfies* $\frac{\partial f_{inner}(\boldsymbol{a},\boldsymbol{b})}{\partial \boldsymbol{w}} = \boldsymbol{0}$*, and* $\frac{\partial^2 f_{inner}(\boldsymbol{a},\boldsymbol{b})}{\partial \boldsymbol{w} \partial \boldsymbol{w}}$ *(i.e., the Jacobian matrix) is invertible. Then, we have the Jacobian matrix of partial derivatives of* $\boldsymbol{w}(\boldsymbol{\lambda})$ *as follows:*

$$\frac{\partial \boldsymbol{w}(\boldsymbol{\lambda})}{\partial \boldsymbol{\lambda}} = -[\frac{\partial^2 f_{inner}(\boldsymbol{\lambda}, \boldsymbol{w})}{\partial \boldsymbol{w} \partial \boldsymbol{w}}]^{-1} \times \frac{\partial^2 f_{inner}(\boldsymbol{\lambda}, \boldsymbol{w})}{\partial \boldsymbol{w} \partial \boldsymbol{\lambda}}.$$

Thus, with the assumption that the inner optimization has converged to a local minimum, i.e., $\frac{\partial f_{\text{inner}}}{\partial \boldsymbol{w}} = 0$, we can convert the best-response Jacobian in Eq. 1 to the multiplication of two matrices in Eq. 2. Similarly, we can convert the best-response Jacobian w.r.t. $\boldsymbol{\mu}$ by setting $F(\boldsymbol{x}, \boldsymbol{y})$ to $\frac{\partial f_{\text{inner}}(\boldsymbol{\mu},\boldsymbol{w})}{\partial \boldsymbol{w}}$ and $G(\boldsymbol{x})$ to $\boldsymbol{w}(\boldsymbol{\mu})$.

A.4 Setting for the Validity Check

Continuing from Sec. 2.2, we describe the synthetic binary setting in Roh et al. (2021), which is used to empirically verify how close the solutions from our approximation strategy are to the optimal ones.

For generating the synthetic dataset, we use a method in Zafar et al. (2017a), which produces two input attributes (x_1, x_2), one binary label attribute y, and one binary group attribute z. We draw each sample (x_1, x_2, y) from Gaussian distributions and make z follow a biased distribution.

In detail, we generate each sample (x_1, x_2, y) from two Gaussian distributions: $(\mathrm{x}_1, \mathrm{x}_2)|\mathrm{y} = 0 \sim \mathcal{N}([-2; -2], [10, 1; 1, 3])$ and $(\mathrm{x}_1, \mathrm{x}_2)|\mathrm{y} = 1 \sim \mathcal{N}([2; 2], [5, 1; 1, 5])$. Then, we make z follow a biased distribution: $\Pr(\mathrm{z} = 1) = \Pr((\mathrm{x}'_1, \mathrm{x}'_2)|\mathrm{y} = 1)/[\Pr((\mathrm{x}'_1, \mathrm{x}'_2)|\mathrm{y} = 0) + \Pr((\mathrm{x}'_1, \mathrm{x}'_2)|\mathrm{y} = 1)]$ where $(\mathrm{x}'_1, \mathrm{x}'_2) = (\mathrm{x}_1 \cos(\pi/4) - \mathrm{x}_2 \sin(\pi/4), \mathrm{x}_1 \sin(\pi/4) + \mathrm{x}_2 \cos(\pi/4))$. This synthetic dataset contains training, validation, and test sets with 2k, 1k, and 1k samples, respectively.

In this experiment, we use logistic regression models for all algorithms, as in Roh et al. (2021).

A.5 Comparison with Exact Inverse Hessian Computation

Continuing from Sec. 2.2, we compare our identity matrix-based approximation results with the exact inverse Hessian computation results. We use the same setting described in Sec. A.4, where it is tractable to compute the exact inverse Hessian.

Figure 4 shows the group ratios of Dr-Fairness (with the identity matrix approximation) and Dr-Fairness with the exact inverse Hessian computation. We can see that Dr-Fairness, which uses the identity matrix approximation to estimate the inverse Hessian in Eq. 2, converges to similar group ratios to those in computing the exact inverse Hessian. It implies that our solution is close to the exact solution despite the method's simplicity. Another observation is that the data ratios in Figure 4b converge within fewer iterations than those in Figure 4a. We note that although the number of required iterations is fewer when computing the exact inverse Hessian, the training time is much slower if the number of parameters increases. Thus, the approximation used in Dr-Fairness can be a reasonable solution to estimate the inverse Hessian, which is usually intractable for large models and data.

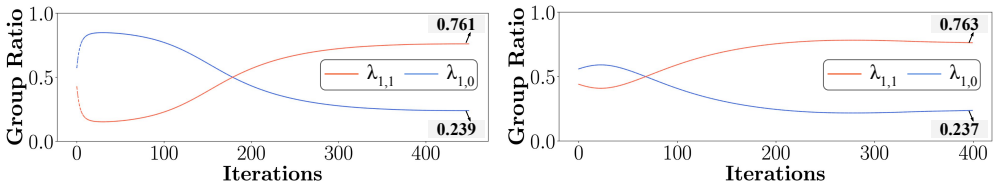

(a) Group ratios in Dr-Fairness. (b) Group ratios with the exact inverse Hessian.

Figure 4: Comparison of group ratios $\boldsymbol{\lambda}$ from Dr-Fairness (with the identity matrix approximation) and Dr-Fairness with the exact inverse Hessian computation. Both converge to similar ratios.

B APPENDIX – EXPERIMENTS

B.1 EXPERIMENTAL SETTINGS

Continuing from Sec. 3, we provide detailed information on the experimental settings. We use PyTorch for all experiments and utilize the pre-trained ResNet50 (He et al., 2016) provided by PyTorch library (i.e., torchvision (Marcel & Rodriguez, 2010)). We change the last fully-connected layer of each model with the number of corresponding label classes. When training, we update all model parameters in the pre-trained model. The batch size of all experiments is 128. We set the learning rate for updating model parameters to 0.0001. For the data ratio ($\boldsymbol{\lambda}$ and $\boldsymbol{\mu}$) updates in Dr-Fairness, we use the Adam optimizer and set the learning rate for the ratio update to 0.005 in all experiments. When calculating the gradients w.r.t. model parameters or data ratios in Eq. 3, we use the autograd functionality in PyTorch. We apply the exponential moving average when updating the model parameters in Dr-Fairness. To prevent the overfitting, we use the validation set when measuring the fairness and accuracy losses in the outer objective of our bilevel optimization. Similarly, we use the validation set in other baselines if they require the computation of additional (fairness) losses in the algorithm.

Hyperparameters For Dr-Fairness, we choose k from a candidate set $\{0.1, 1, 10, 20\}$ to have the best fairness score while minimizing the accuracy degradation in the validation set. We set the learning rates for $\boldsymbol{\lambda}$ and $\boldsymbol{\mu}$ to 0.005. We initialize $\boldsymbol{\lambda}$ to the original (y, z)-ratios in the real data. We initialize $\boldsymbol{\mu}$ to 0.5 for CelebA (i.e., we start with 50% real and 50% generated data) and 0.99 for ImageNet People Subtree (i.e., 99% real and 1% generated data). We use a higher (conservative) $\boldsymbol{\mu}$ initially for ImageNet People Subtree because its generated data has lower quality than that for CelebA. For all baselines, we choose the hyperparameters that show the best fairness while minimizing the accuracy degradation in the validation set.

B.2 FILTERING LABEL CLASSES IN IMAGENET PEOPLE SUBTREE

Continuing from Sec. 3, we explain how we filter the label classes in the ImageNet People Subtree dataset. Initially, the dataset contains 284 label classes. Among them, we filter out classes that are vague, duplicates, or too small with few samples. First, we filter vague classes like "ex-president" and "junior", which are hard to classify even for human annotators. To decide whether each class is vague or not, we perform internal crowdsourcing. For each class, we gather 3 expert decisions and do a majority vote. Also, we remove classes that are conceptually duplicates of others. Finally, we set the allowed minimum sample size to 50 and ignore the classes with fewer than 50 samples. As a result, 112 classes are used in our experiments.

B.3 DATA GENERATION

Continuing from Sec. 3, we explain the details on data generation.

For experiments on CelebA, we use LACE (Nie et al., 2021) to generate data. LACE is a controllable generation method that uses an energy-based model (EBM) in the latent space of a pre-trained generative model such as StyleGAN2 (Karras et al., 2020). We consider StyleGAN2 pre-trained on the CelebA-HQ dataset as our base generative model. In LACE, we first need to train the latent classifiers in the w-space of StyleGAN2, each of which corresponds to an energy function for an individual attribute in the EBM formulation (see Eq. (4) in (Nie et al., 2021)). Since we mainly focus on five attributes (i.e., `age`, `gender`, `smile`, `glasses`, and `haircolor`) in the CelebA experiments, we end up with five latent classifiers. Next, for each combination of attribute values (e.g., `age`='young', `gender`='female', `smile`='true', `glasses`='true', and `haircolor`='black'), we use the ordinal differential equation (ODE) sampler in the latent space to sample the corresponding images. We repeat the above sampling process until we cover all the combinations of attribute values.

For experiments on ImageNet People Subtree, we use a guided diffusion model (Dhariwal & Nichol, 2021) with classifier guidance (Song et al., 2020; Dhariwal & Nichol, 2021) to generate data. Since there exist no ADM checkpoints pre-trained on ImageNet People Subtree, we first fine-tune

the ImageNet-pretrained ADM on ImageNet People Subtree, where the ADM model that we use conditions on the 112 labels. For classifier guidance, we also need to first train three time-dependent attribute classifiers, each corresponding to a demographic attribute (i.e., `gender`, `skin color`, and `age`), on noisy images produced by the diffusion process. In particular, we fine-tune the noisy image classifier (also pre-trained on ImageNet) with three new prediction heads on 10% of the annotated data. Next, for each combination of label and attribute values, we pass the label value as the input of the conditional ADM and use the classifier guidance (i.e., the guidance from the fine-tune noisy image classifier in Eq. (10) of Dhariwal & Nichol (2021)) with the scale $s = 15$. Similarly, we repeat the above sampling process until we cover all the combinations of label and attribute values.

Here we describe the number of generated samples in each dataset. In CelebA, we consider 5 attributes for the controllable generation: `gender` (male and female), `age` (young and old), `smile` (true and false), `glasses` (true and false), and `haircolor` (black, blond, and others). Thus, these 5 attributes yield 48 class combinations (i.e., $2^4 \times 3$). We generate a total of 96k samples, where there are 2k samples for each attribute combination (e.g., 2k samples for (`age`='young', `gender`='female', `smile`='true', `glasses`='true', and `haircolor`='black')). In ImageNet People Subtree, there are 112 label classes and 3 group attributes: `gender` (male, female, and unsure), `skin color` (light, medium, and dark), and `age` (child, adult, middle, and retired). Thus, we have 4,032 combinations (i.e., $112 \times 3 \times 3 \times 4$) for the controllable generation. We generate 32 samples for each combination, which results in about 129k samples in total.

Figures 5 and 6 show examples of the generated images. We note that the controllable generation for ImageNet People Subtree is more challenging due to its large number of (y, z)-classes and labeling noises. Thus, the resulting generated data is noisier than the generated data in CelebA.

Figure 5: Examples of the generated images on CelebA.

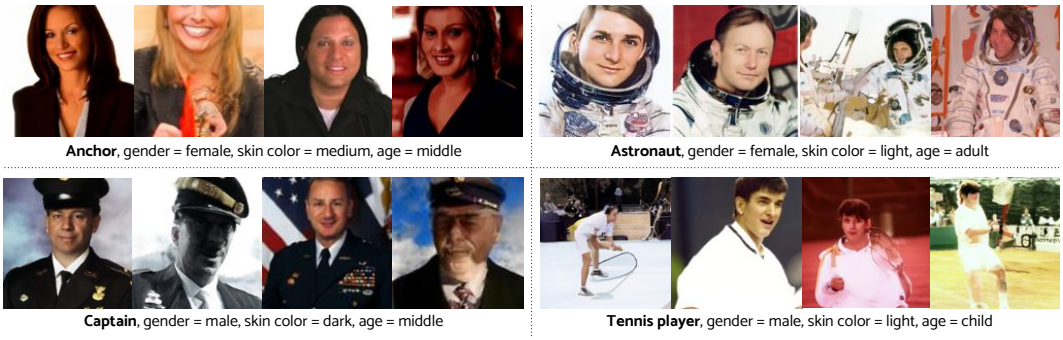

Figure 6: Examples of the generated images on ImageNet People Subtree.

B.4 Comparison between FairnessGAN and PairAug

Continuing from Sec. 3.1.1, we compare FairnessGAN (Sattigeri et al., 2019) and PairAug (Ramaswamy et al., 2021). Table 6 shows the accuracy and fairness performances of the two algorithms on CelebA, where they consider the setting of binary label attribute y (attractive) and binary group

attribute z (gender). We show the numbers that are reported in Ramaswamy et al. (2021). As a result, PairAug shows better accuracy and equalized odds performances compared to FairnessGAN.

Table 6: Additional comparisons between baselines using generated data. We compare PairAug and FairnessGAN, where the results are from Ramaswamy et al. (2021). The baselines use the *attractive* attribute as the label and *gender* attribute as the group.

Method	Acc.	EO Disp.
PairAug (Ramaswamy et al., 2021)	**80.0**	**0.21**
FairnessGAN (Sattigeri et al., 2019)	71.0	0.25

B.5 Other Results on CelebA w.r.t. Demographic Parity

Continuing from Sec. 3.1.1, we perform experiments on the CelebA dataset w.r.t. demographic parity (DP). Table 7 shows the accuracy and fairness performances of the algorithms. Similar to the results in Table 2, Dr-Fairness shows higher fairness than the pre-processing (1:1 data ratio) baselines (i.e., simple sampling, PairAug, and PairAug*) and higher accuracy than the in-processing baselines (i.e., fairness constraint, domain independence, and FairBatch). Here, as the pre-processing baselines are not explicitly designed for DP, their fairness performances in terms of DP are sometimes worse than the original ResNet50 results. Since DP aims to ensure the same positive prediction rates without considering the true labels, the training sometimes needs to overfit on the positive labels for specific groups to improve DP. Thus, simply equalizing the data ratio among groups may not be enough to improve DP compared to the EO case.

Table 7: Performances on the CelebA test set w.r.t. demographic parity (DP) on the binary y (age) and z (gender) scenario. Other settings are identical to Table 2. We mark the best and second best performances among the fairness algorithms with bold and underline, respectively.

	y: age and z: gender			
Method	Acc.	Bal. Acc.	DP Disp.	Bias Amp.
Non-fair	86.4$\pm$0.3	76.4$\pm$0.2	0.141$\pm$0.009	0.101$\pm$0.022
Simple Sampling	**86.8$\pm$0.2**	78.3$\pm$0.5	0.132$\pm$0.010	0.052$\pm$0.017
PairAug (Ramaswamy et al., 2021)	85.6$\pm$0.6	**79.8$\pm$0.3**	0.151$\pm$0.007	0.030$\pm$0.006
PairAug* (Ramaswamy et al., 2021)	<u>86.7$\pm$0.2</u>	<u>79.3$\pm$0.6</u>	0.144$\pm$0.003	0.053$\pm$0.008
Fair. Const. (Zafar et al., 2017a)	85.9$\pm$0.3	74.3$\pm$1.3	0.124$\pm$0.009	0.103$\pm$0.006
Dom. Indep. (Wang et al., 2020)	85.0$\pm$0.7	72.4$\pm$2.1	0.091$\pm$0.004	0.034$\pm$0.021
FairBatch (Roh et al., 2021)	84.9$\pm$0.3	74.0$\pm$1.5	**0.074$\pm$0.005**	**-0.034$\pm$0.004**
Dr-Fairness	86.5$\pm$0.3	78.2$\pm$0.1	<u>0.088$\pm$0.009</u>	<u>-0.028$\pm$0.005</u>

B.6 Other Results on CelebA with Different Settings

Continuing from Sec. 3.1.1, we perform experiments on the CelebA dataset with different group and label combinations. Tables 8 and 9 show the accuracy and fairness performances on the following two settings: (y, z) = (smiling, gender) and (y, z) = (haircolor, gender). In both cases, we observe consistent results to those in Sec. 3.1.1, where Dr-Fairness achieves high fairness (esp. EO) while not sacrificing accuracy. We note that in these two settings, the bias amplification values of the non-fair baseline are already very small (i.e., good enough), so the fair algorithms may not further improve the bias amplification.

B.7 Accuracy-Fairness Tradeoffs

Continuing from Sec. 3, we visually demonstrate the accuracy-fairness tradeoffs of Dr-Fairness and the baselines on the CelebA and ImageNet People Subtree datasets. Figure 7 shows the accuracy and

Table 8: Performances on the CelebA test set w.r.t. equalized odds (EO) on the binary y (smiling) and binary z (gender) scenario. We mark the best and second best performances among the fairness algorithms with bold and underline, respectively. Other settings are identical to Table 2.

	z: age			
Method	Acc.	Bal. Acc.	EO Disp.	Bias Amp.
Non-fair	91.7±0.2	91.7±0.2	0.027±0.004	0.006±0.002
Simple Sampling	91.8±0.1	91.8±0.1	0.019±0.007	0.012±0.004
PairAug (Ramaswamy et al., 2021)	91.4±0.1	91.4±0.1	0.022±0.001	**0.003±0.001**
PairAug* (Ramaswamy et al., 2021)	92.0±0.1	92.0±0.1	0.031±0.001	**0.003±0.000**
Fair. Const. (Zafar et al., 2017b)	91.3±0.5	91.3±0.5	0.014±0.007	0.009±0.002
Dom. Indep. (Wang et al., 2020)	91.2±0.3	91.2±0.3	0.014±0.000	0.009±0.004
FairBatch (Roh et al., 2021)	91.6±0.1	91.6±0.1	**0.012±0.002**	0.018±0.002
Dr-Fairness	**92.7±0.1**	**92.7±0.1**	0.013±0.003	0.009±0.004

Table 9: Performances on the CelebA test set w.r.t. equalized odds (EO) on the non-binary y (haircolor) and binary z (gender) scenario. We mark the best and second best performances among the fairness algorithms with bold and underline, respectively. Other settings are identical to Table 2.

	y: haircolor and z: gender			
Method	Acc.	Bal. Acc.	EO Disp.	Bias Amp.
Non-fair	83.8±0.3	82.0±0.6	0.399±0.019	0.010±0.003
Simple Sampling	83.1±0.1	78.9±0.8	0.322±0.006	0.021±0.004
PairAug* (Ramaswamy et al., 2021)	82.7±0.9	80.0±3.0	0.374±0.029	0.018±0.013
Dom. Indep. (Wang et al., 2020)	83.2±0.2	79.4±0.9	0.308±0.033	**0.011±0.006**
FairBatch (Roh et al., 2021)	78.4±1.4	68.7±1.3	0.085±0.015	0.072±0.022
Dr-Fairness	**84.5±0.2**	**82.3±0.7**	**0.029±0.009**	0.023±0.009

unfairness performances of the baselines and Dr-Fairness. Here, being on the lower-right indicates higher accuracy and fairness and is thus desirable. In CelebA, Dr-Fairness achieves both better accuracy and fairness performances compared to all the baselines. In ImageNet People Subtree, 1) the baselines Simple Sampling, PairAug, and Dom. Indep. show strictly worse performances than Dr-Fairness, 2) FairBatch achieves higher fairness than ours, but the accuracy degradation is severe, and 3) the non-fair baseline shows high accuracy, but much worse fairness. Thus, we can conclude that Dr-Fairness achieves the best accuracy-fairness tradeoffs in both datasets.

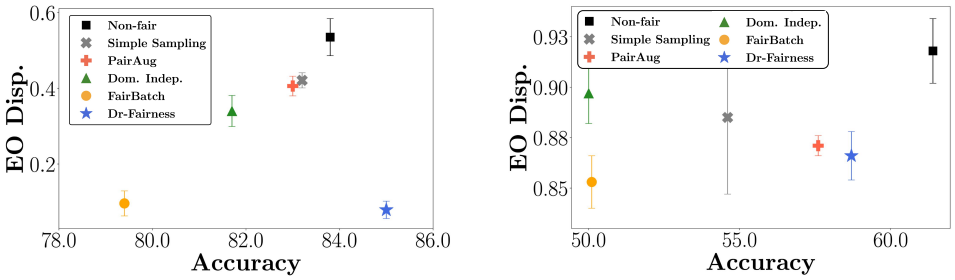

(a) Tradeoffs in CelebA when (y, z) = (haircolor, (gender, age)).

(b) Tradeoffs in ImageNet People Subtree when z = (gender, skin color, age).

Figure 7: Accuracy-unfairness graphs to visualize the algorithm performances on the CelebA and ImageNet People Subtree datasets. Being on the lower right is desirable (high accuracy and fairness).

We explain when Dr-Fairness can improve *both* fairness and accuracy compared to other fairness baselines. We believe this phenomenon is related to the optimal accuracy-fairness tradeoff, which is known to be determined by the data distribution (Menon & Williamson, 2018). When the performance of a fair algorithm lies on the optimal accuracy-fairness tradeoff, any other algorithm can only achieve

either better fairness or better accuracy, but cannot improve both. However, when the fairness algorithms do not achieve the optimal accuracy-fairness tradeoff in the given data, there is an opportunity to improve the model's performances toward the optimal tradeoff line. For example, we observe that Dr-Fairness improves both accuracy and fairness compared to other baselines in CelebA, implying that the baselines do not achieve the optimal accuracy-fairness tradeoff in the first place.

B.8 Other Results on ImageNet People Subtree with Different Groups

Continuing from Sec. 3.2, we perform experiments on the ImageNet People Subtree with different groups. Table 10 shows the accuracy and fairness performances when the group attribute is gender or skin color. We observe consistent results to those in Sec. 3.2.

Table 10: Performances on the ImageNet People Subtree test set when training w.r.t. equalized odds (EO) for either gender or skin color. We mark the best and second best performances among the fairness algorithms with bold and underline, respectively. Other settings are identical to Table 2.

	z: gender				z: skin color			
Method	Acc.	Bal. Acc.	EO Disp.	Bias Amp.	Acc.	Bal. Acc.	EO Disp.	Bias Amp.
Non-fair	61.4±0.8	61.8±0.8	0.871±0.013	0.256±0.031	61.4±0.8	61.8±0.8	0.874±0.024	0.239±0.062
Simple Sampling	54.8±0.8	54.9±0.9	0.834±0.004	0.282±0.038	55.5±1.1	55.7±1.0	0.849±0.000	0.219±0.035
PairAug* (Ramaswamy et al., 2021)	54.6±0.5	54.9±0.5	0.821±0.030	0.241±0.034	58.1±0.1	58.3±0.1	0.830±0.000	0.225±0.010
Dom. Indep. (Wang et al., 2020)	**59.9±0.1**	**60.1±0.1**	0.857±0.016	0.381±0.033	60.2±0.2	60.5±0.3	0.874±0.009	0.204±0.009
FairBatch (Roh et al., 2021)	52.9±3.1	53.1±3.2	**0.816±0.076**	**0.191±0.011**	51.9±0.5	52.1±0.5	**0.811±0.019**	0.346±0.021
Dr-Fairness	58.2±0.3	58.3±0.2	0.817±0.012	0.220±0.027	**60.8±1.4**	**61.2±1.3**	0.845±0.001	**0.137±0.009**

B.9 Other Results on ImageNet People Subtree with ViT

Continuing from Sec. 3.2, we perform experiments using DeiT-S (Touvron et al., 2021), a variant of ViT (Dosovitskiy et al., 2021), on the ImageNet People Subtree dataset w.r.t. the age group attribute. Table 11 shows the accuracy and fairness performances of Dr-Fairness and the representative baselines. Here we observe similar results to those in Sec. 3.2. This experiment shows that Dr-Fairness is applicable to various network architectures, including ViT.

Table 11: Performances on the ImageNet People Subtree test set w.r.t. equalized odds (EO). We use DeiT-S (Touvron et al., 2021), a variant of ViT (Dosovitskiy et al., 2021), for all algorithms. We mark the best and second best performances among the fairness algorithms with bold and underline, respectively. Other settings are identical to Table 2.

	z: age			
Method	Acc.	Bal. Acc.	EO Disp.	Bias Amp.
Non-fair	64.8±0.0	65.2±0.1	0.890±0.027	0.198±0.030
Simple Sampling	55.3±0.7	55.7±0.7	0.807±0.011	0.261±0.081
PairAug* (Ramaswamy et al., 2021)	59.5±0.1	59.9±0.1	0.824±0.006	0.237±0.083
Dom. Indep. (Wang et al., 2020)	51.8±1.6	52.0±1.5	0.817±0.005	0.634±0.246
FairBatch (Roh et al., 2021)	58.2±0.6	58.6±0.5	0.817±0.001	**0.162±0.016**
Dr-Fairness	**64.4±0.6**	**64.8±0.6**	**0.774±0.001**	0.176±0.001

C APPENDIX – RELATED WORK

Continuing from Sec. 4, we discuss more related work.

The main approaches for satisfying group fairness are: 1) fix the training data to mitigate bias (Kamiran & Calders, 2011; Zemel et al., 2013), 2) modify the training process to prevent the model from learning bias (Zafar et al., 2017a;b; Zhang et al., 2018a; Agarwal et al., 2018; Roh et al., 2020; 2021), or 3) alter the outputs of the trained model to achieve fairness metrics (Hardt et al., 2016). As discussed in Sec. 4, most of these algorithms are not designed to handle large number of groups or labels, and our contribution is to support such large-scale scenarios for real-world applications.

In addition, there are other related studies on 1) fair data reweighing (Li & Liu, 2022; Jiang & Nachum, 2020; Krasanakis et al., 2018), 2) fair augmentation (Chuang & Mroueh, 2021), and 3) fair representations (Shui et al., 2022).

- The data reweighing techniques (Li & Liu, 2022; Jiang & Nachum, 2020; Krasanakis et al., 2018) are indeed relevant to our data sampling framework, as they keep finding data weights to improve group fairness. Compared to our work, Jiang & Nachum (2020) and Krasanakis et al. (2018) require multiple re-training of the model, and Li & Liu (2022) uses additional assumptions, including the loss function being twice differentiable and strictly convex in the model parameters. Therefore, applying these reweighing techniques when training models on large-scale data may lead to significant training times due to multiple re-trainings or performance degradation due to violations of the assumptions. In comparison, Dr-Fairness works well in large-scale scenarios as in our experiments.
- There is another interesting work called FairMixup (Chuang & Mroueh, 2021), which augments training data for fairness using mixup methods (Zhang et al., 2018b). However, the key difference from ours is that FairMixup only augments the data within the original training data distribution. FairMixup also cannot dynamically adjust sampling ratios from different groups explicitly. In contrast, Dr-Fairness can utilize any additional data, which is not limited to the original training (real) data distribution, and also find the optimal sampling ratios among groups and between real and generated data.
- Recently, a fair representation paper (Shui et al., 2022) uses the bilevel optimization formulation and shows promising results. Although this work also uses a bilevel formulation, it targets a different problem from ours, where the goal is to map the input feature X into the latent variable X' for fairness. In comparison, we use the bilevel formulation to adjust the ratio among groups and between real and generated data to improve fairness.

Although not our immediate focus, there are other important research lines for fairness: 1) fulfilling other fairness definitions (e.g., individual fairness (Dwork et al., 2012) and causal fairness (Kusner et al., 2017)) and 2) handling noisy or missing group labels (Hashimoto et al., 2018; Celis et al., 2021). We believe that supporting these aspects can be promising future directions.